Growth Inhibition of Osteosarcoma Cell Lines in 3D Cultures: Role of Nitrosative and Oxidative Stress

MAGDALENA GORSKA[1], PAWEL BIENIASZ KRZYWIEC[2], ALICJA KUBAN-JANKOWSKA[1], MICHAL ZMIJEWSKI[2], MICHAL WOZNIAK[1], JUSTYNA WIERZBICKA[2], ANNA PIOTROWSKA[2] and KAROLINA SIWICKA[1,3]

Departments of [1]Medical Chemistry, and [2]Histology, Medical University of Gdansk, Gdansk, Poland; [3]Department of Kinesiology, Gdansk University of Physical Education and Sport, Gdansk, Poland

Abstract. *Background: 3D cell cultures have revolutionized the understanding of cell behavior, allowing culture of cells with the possibility of resembling in vivo intercellular signaling and cell–extracellular matrix interaction. Aim: The effect of limited oxygen penetration into 3D culture of highly metastatic osteosarcoma 143B cells in terms of expression of nitro-oxidative stress markers was investigated and compared to standard 2D cell culture. Materials and Methods: Human osteosarcoma (143B cell line) cells were cultured as monolayers, in collagen and Matrigel. Cell viability, gene expression of nitro-oxidative stress markers, and vascular endothelial growth factor were determined using Trypan blue assay, quantitative polymerase chain reaction and enzyme-linked immunosorbent assay, respectively. Results: Three-dimensional environments modify nitro-oxidative stress and influence gene expression and cell proliferation of OS 143B cells. Conclusion: Commercial cell lines might not constitute a good model of 3D cultures for bone tissue engineering, as they are highly sensitive to hypoxia, and hypoxic conditions can induce oxidation of the cellular environment.*

Monolayer (2D) culture of various osteoblast-like cell lines has for many decades played a key role in the investigation of bone physiology and pathology. Although useful, 2D cultures do not mimic the bone-tissue environment faithfully. Cells cultured *in vitro* (whether for basic research or for tissue engineering and clinical application) experience unfavorable conditions that are uncommon *in vivo*. *In vivo* rarely do cells (especially osteoblast-like cells) grow in monolayers. Cell culture does not reflect the spatial organization between the cell and the extracellular matrix (ECM), and the complexity of cell-to-cell interactions – the key to natural cell processes.

Recently, the evolving models of 3D cell culture has opened up new dimensions in cell-based assays and tissue engineering (1). 3D cell cultures have revolutionized our understanding of cell behavior through providing cultured cells with the possibility of resembling *in vivo* intercellular signaling and cell–ECM interaction. Various spatial cultures for osteoblastic-like lines have been proposed (2). Cells may grow within self-produced ECM in micromasses (3) or in spheroid cultures (4), on synthetic-based polymers (5), calcium phosphate ceramics (6), in externally delivered matrices such as collagen type I (7, 8), Matrigel (9), or in combination with other scaffolds (10). The striking similarity of *in vivo* morphologies and behaviors of cells grown in 3D cultures have been well-documented (11). Encapsulation of cells within a hydrogel could improve their viability by providing biomechanical protection, biochemical survival cues and scaffolding. On one hand, spatial cell cultures are being accused of being unreliable because of an uneven distribution of metabolic substrates and products, irregular gas penetration within the scaffold, as well as of substantial hypoxia (12, 13) (compared to a classic hyperoxic cell culture, but not when compared to *in vivo* conditions). However, on the other hand, processes within living organisms never proceed evenly, undisturbed and symmetrically, thus such inconsistences should be considered physiological. At the same time, some reports suggest that pericellular matrices in spatial scaffolds can actually serve as natural defense mechanisms against free radicals and reactive oxygen species (14).

Nitro-oxidative stress is an underappreciated problem in *ex vivo* investigations of cell physiology and pathology. Various

Correspondence to: Magdalena Gorska or Karolina Siwicka or Michal Zmijewski, Department of Medical Chemistry, Medical University of Gdansk, Dębinki 1, Gdansk 80-211, Poland. Tel: +48 3491450, Fax: +48 3491456, e-mail: m.gorska@gumed.edu.pl, karolinasiwicka@gumed.edu.pl, mzmijewski@gumed.edu.pl

Key Words: Extracellular matrix, ECM, monolayer/spatial (2D/3D) cell culture, OS 143B cell line, nitro-oxidative stress.

studies demonstrated that the use of universal 2D cell culture modulates cell proliferation, growth, differentiation, intra- and intercellular signaling and produces cell behavior distinct form that *in vivo*. It is widely known that *in vitro* incubation exposes cultured lines to partial oxygen pressure many times higher than that found within a living organism, moreover, cells cultured in a traditional monolayer model are deprived of the spatial organization between cells themselves and between cells and ECM characteristic for them – the key to natural cell processes.

Herein, we aimed to investigate the effects of a novel 3D osteosarcoma 143B cellular model on cell growth and expression of nitro-oxidative stress markers within the cultures. We have also correlated the nitro-oxidative stress levels in 3D cultures with growth factor signal transduction, cell viability, proliferation and intercellular interactions in the cultures.

Materials and Methods

Cell line and culture conditions. Human osteosarcoma cell line143B (ATCC® CRL-8303™) derived from a primary osteogenic sarcoma were used in the experiments. For 2D culture, osteosarcoma cells were seeded at a density of 6×10^4 cells/cm^2. For 3D culture, cells were seeded in either collagen gel or Matrigel at a density of 10^6 cells per 1 ml of scaffold and following the full gelation of the scaffold. The cells were cultured at 37˚C in a humidified atmosphere saturated with 5% CO_2 using Dulbecco's modified Eagle's medium supplemented with 10% heat-inactivated fetal bovine serum and a penicillin (100 mg/ml)/streptomycin (100 mg/ml) cocktail (Sigma-Aldrich, St. Louis, MO, USA).

Collagen matrix. Collagen gels were prepared by mixing a chilled solution of collagen type I from bovine skin and tendon (C4243; Sigma-Aldrich) with phosphate buffered saline (PBS) 10x, fetal bovine serum, 200 mM L-glutamine solution (G7513; Sigma-Aldrich), penicillin-streptomycin, and supplemented with 7.5% sodium bicarbonate (S5761; Sigma-Aldrich) solution to adjust pH of the mixture to 7.2-7.6. The prepared collagen solution was used to firstly coat wells of the culture dish with a 0.5 mm-thick collagen layer. The culture dish was incubated at 37˚C for about 30 min to allow gel formation. This thin layer prevented cells plated in the following step from migrating and adhering to the bottom of the culture dish. The osteosarcoma cells suspended in a minimal amount of medium were mixed with the remaining collagen solution and plated on the top of the collagen-coated culture dish to form a collagen layer of a total of 1 mm thickness. The plate was incubated again at 37˚C and after complete gelation, cell culture medium was added.

Matrigel matrix. Matrigel (BD Biosciences, Bedford, MA, USA) was thawed overnight on ice. All procedures were carried out on ice. Matrigel was placed in multiple-well plates to form coatings of approximately 1 mm in thickness. Immediately after Matrigel transfer, cell suspensions were added to the Matrigel-covered wells and mixed with Matrigel. Cells were added to Matrigel to be seeded in a final density of approximately 10^6 cells per 70 mm^3 of the scaffold. Next, plates were placed in an incubator to allow Matrigel solidification at 37˚C (around 5 min). After gelation, cell culture medium was added to the Matrigel-coated wells to form approximately 5-mm-thick layer above the cell-seeded scaffolds.

Trypan blue exclusion test of cell viability. Osteosarcoma 143B cells were harvested from monolayer cultures using Trypsin-EDTA (59418C; Sigma-Aldrich), from collagen scaffold using collagenase from *Clostridium hystoliticum*, type H (C8051; Sigma-Aldrich) (1 mg/1 ml of collagen in physiological solution) and from Matrigel using minimal digestion with Accutase (Millipore, Billerica, MA, USA) after 24, 48 or 72 h of cell culture and stained with 0.4% Trypan blue dye (Sigma-Aldrich) for 3 min. Trypan blue-positive and -negative cells were counted with a BLAUBRAND® counting chamber (BRAND, Wertheim, Germany) under a phase-contrast microscope (CKX41; Olympus, Glasgow, UK). The experiments were performed in triplicates.

Light microscopical analysis. 143B osteosarcoma cells cultured in three different environments (2D, 3D- Collagen, Matrigel) were photographed at different time points by light phase-contrast microscopy at ×20 magnification using Quick Photo Camera 2.3 (PROMICRA, Prague, Czech Republic) software. For imaging, a CKX41 inverted microscope (Olympus) was employed.

RNA extraction and real time polymerase chain reaction (PCR) analysis. Reverse transcription (1 μg RNA/reaction) was performed as previously described (15) with First Strand cDNA Synthesis Kit (Thermo Scientific, Waltham, MA, USA) according to the manufacturer's protocol (16). Real-time PCR reactions were performed with the initial denaturation at 95˚C for 5 min (phase I) and then 40 cycles at 95˚C for 15 s, 57˚C for 60 s and 72˚C for 20 s, ending with fluorescence reading at 78˚C for 10 s. Then melting curve stage started at 95˚C for 15 s, next cooling to 70˚C for 60 s with temperature increasing to 95˚C and fluorescence read each 0.3˚C. The primers were designed using primer-blast algorithm at www.ncbi.nlm.nih.gov on the basis of Refseq mRNA database option. Real-time PCR reactions were performed with Applied Biosystems StepOnePlus Real-Time PCR thermocycler and analyzed using Step One Software (Applied Biosystems, Foster City, CA, USA). Results obtained for the gene of interest were normalized against ribosomal protein L 37a (*RPL37A*) reference gene. Subsequently, the values were related to the control sample (set to 1). All qPCR reactions were repeated at least three times to ensure the replicability of the results. The primers used are shown in Table I.

Enzyme-linked immunosorbent assays (ELISA). ELISA was performed to measure the concentration of vascular endothelial growth factor (VEGF) in cell culture media of 143B cells. VEGF level was measured using ELISA kits, according to the manufacturer's instructions (Sigma-Aldrich). All standards and samples were run in triplicates. The mean absorbance for each set of duplicate standards and samples was calculated and the average zero standard optical density was subtracted. The standard curve was plotted using the Microsoft Excel software, and the best-fit curve was drawn through the standard points.

Statistical analysis. The results are presented as the mean±standard deviation (SD) of values obtained from at least three independent experiments. The statistical significance of the differences was analyzed by the two-tailed *t*-test. A *p*-value of less than 0.01 was considered to correspond to statistical significance. Data were

Table I. *Primers used for polymerase chain reaction analysis*.

Gene	Protein name	Primer sequences (5' → 3')
RPL37A	60S ribosomal protein L37a	F: TTCTGATGGCGGACTTTACC R: CACTTGCTCTTTCTGTGGCA
SOD1	Superoxide dismutase 1	F: CCACACCTTCACTGGTCCAT R: CTAGCGAGTTATGGCGACG
SOD2	Superoxide dismutase 2	F: TAGGGCTGAGGTTTGTCCAG R: CACCGAGGAGAAGTACCAGG
CAT	[atalase	F: ACGGGGCCCTACTGTAATAA R: AGATGCAGCACTGGAAGGAG
HSP60	Heat-shock protein 60 kDa	F: TTGCTACTGGTGGTGCAGTGTTTG R: GCATGGCATCGTCTTTGGTCACAA
HSP90AA1	Heat-shock protein 90kDa alpha (cytosolic), class A member 1	F: AGGTTGAGACGTTCGCCTTTCA R: AGATATCTGCACCAGCCTGCAA
HSP90AB1	Heat-shock protein 90kDa alpha (cytosolic), class B member 1	F: AGGAACGTACCCTGACTTTGGT R: ATGCCAATGCCTGTGTCTACCA
HIF1A	Hypoxia-inducible factor 1 alpha	F: GAAAGCGCAAGTCTTCAAAG R: TGGGTAGGAGATGGAGATGC
nNOS	Nitric oxide synthase 1	F: ATTGCCAGCCTGTTAGATGC R: CATATTTATGCCGCGTTTCC
iNOS	Nitric oxide synthase 2	F: ACGGCTCCTTCAAAGAGGCAAA R: TAACGCACGTGTCTGCAGATGT
NOS1AP	Nitric oxide synthase 1 adaptor protein	F: TTGCTGCAGAACAAGGACATGC R: ATGCCTGACTCTCGGAACTTGA

analyzed using Microsoft® Office Excel 2007 (Microsoft, Redmond, WA, USA) and using GraphPad Prism, version 6 (GraphPad Software, Inc., La Jolla, CA, USA).

Results

Trypan blue exclusion test of cell viability. The Trypan blue dye exclusion method was used to measure the cell viability in three different environments (in monolayers, collagen and Matrigel) at various time points. As shown in Figure 1, the percentage of viable 143B cells stayed at the same level in 2D, Matrigel and collagen after 12 and 24 h. After 48 h, the viability of cells in monolayers decreased (82.95%), whereas it was relatively high for Matrigel (91.82%) and collagen (90.46%)-seeded cells. The difference in cell viability between 2D and 3D environments was even sharper after 72 h, when it stayed at the same level in 3D scaffolds (90.88% in Matrigel and 90.82% in collagen) and dropped in monolayers to the level of 78.22%.

Next, the morphology of 143B cells cultivated in 2D, collagen or Matrigel was examined using light microscopy, as shown in Figure 2. 143B cells cultured in monolayers exhibited typical flatten shapes, whereas cells cultured in collagen were narrower and seemed to interact with each other. In contrast, Matrigel-seeded cells had round morphologies and did not proliferate (Figure 2).

Nitro-oxidative stress-related gene expression in 143B human OS cell line. We determined the gene expression of nitro-oxidative stress markers namely: major heat-shock proteins (HSPs): HSP60, HSP90 isoforms; nitric oxide synthases (NOSs) neuronal nNOS, induced iNOS; catalase (CAT) and superoxide dismutase (SOD) isoforms SOD1 and SOD2 by real-time PCR. We have chosen 12 h as zero point in order to allow for total environment stabilization of collagen and Matrigel.

As shown in Figure 3, the expression of mRNA of HSPs was clearly regulated by environmental conditions in which cells were cultivated. For example, transcripts of *HSP60* were strongly down-regulated in cells grown in Matrigel and Collagen after 24, 48 and 72 h when compared to cells in monolayers. The mRNA levels were decreased by ~80-fold after 24 h, ~6-fold after 48 h and ~40-fold after 72 h in Matrigel-seeded cells. This tendency was similar in collagen-seeded cells with the following down-regulation levels: by ~40-fold after 12 h, ~20-fold after 48 h and ~130-fold after 72 h. The effect was also significant for *HSP90AA1* transcripts, with a comparable expression level in all three environments after 12 h and apparent down-regulation at further time points in 3D scaffolds, *e.g.* by ~90-fold after 24 h, ~2.5-fold after 48 h and ~14-fold after 72 h in Matrigel and by ~12-fold after 24 h, ~7-fold after 48 h and ~33-fold after 72 h in collagen. Interestingly, the expression of *HSP90AB1* was generally low in all three environments, but its down-regulation was clear in 3D scaffolds (with the strongest effects in Matrigel).

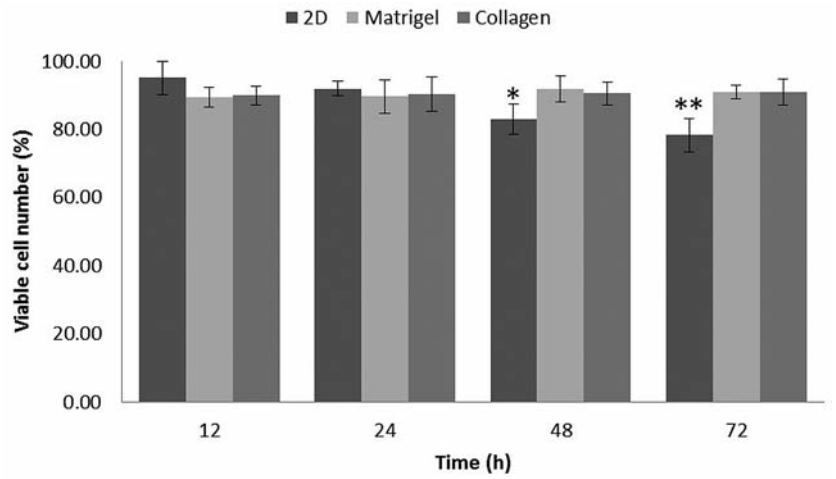

Figure 1. *Viability of 143B human osteosarcoma cells seeded in monolayers (2D) and in 3D scaffolds (Matrigel or collagen) measured by the Trypan blue exclusion assay. The bars show the percentage of viable cells at given time points in different environments. Data are shown as the mean±SD of three independent experiments (N=6 replicate cultures). The absence of an error bar denotes a line thickness greater than the error. *p<0.01 and **p<0.001 versus control (cells at 12 h).*

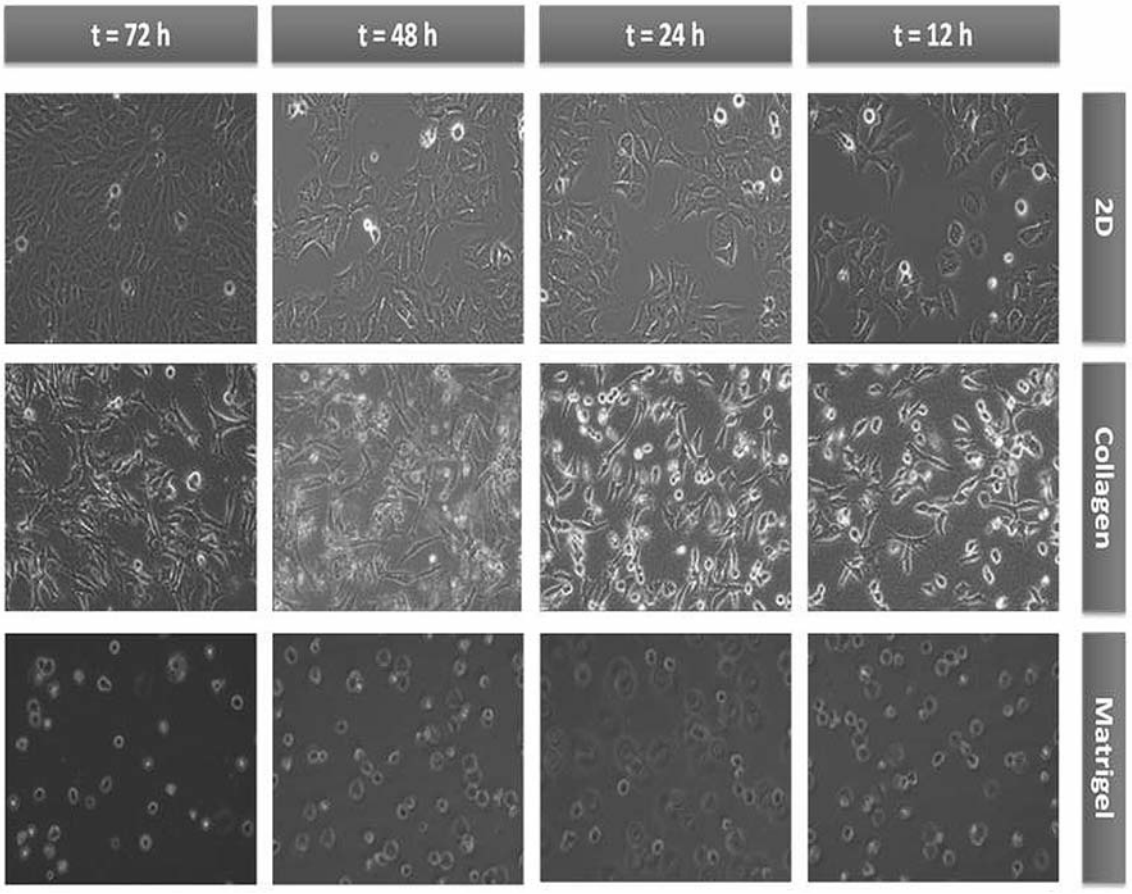

Figure 2. *Morphology and cellular interactions of 143B human osteosarcoma cells cultured in 2D, collagen or Matrigel after 12, 24, 48 or 72 h. Magnification, ×20.*

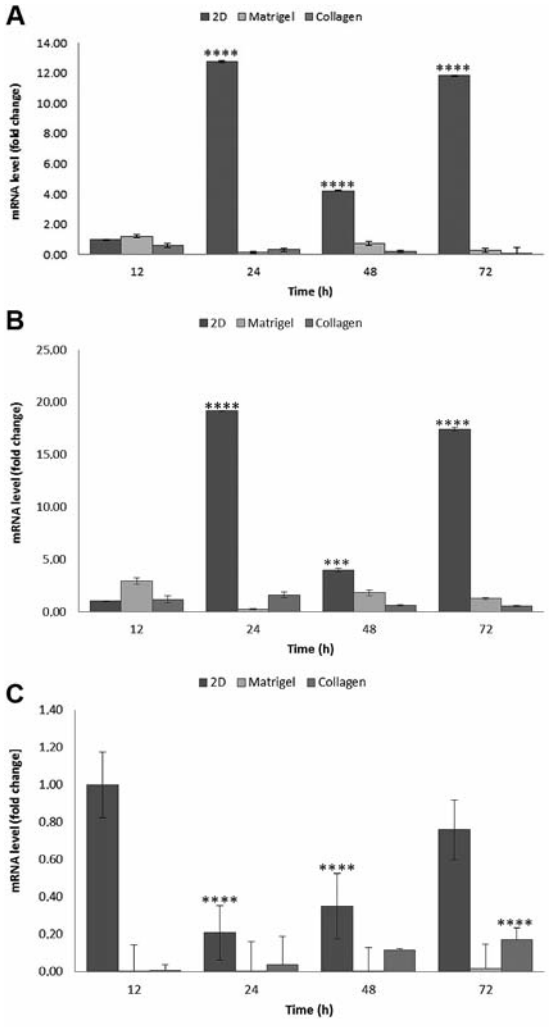

Figure 3. *Expression of mRNA of heat shock protein (HSP)60 (A), HSP90AA1 (B) and HSP90AB1 (C) in 143B human osteosarcoma cells seeded in monolayers (2D) or in 3D scaffolds (Matrigel and collagen) measured by real-time polymerase chain reaction. The results were normalized to the ribosomal protein L 37a (RPL37A) content. Data are shown as the mean±SD of three independent experiments (N=6 replicate cultures). The absence of an error bar denotes a line thickness greater than the error. ***p<0.0001and ****p<0.00001 versus control (cells at 12 h).*

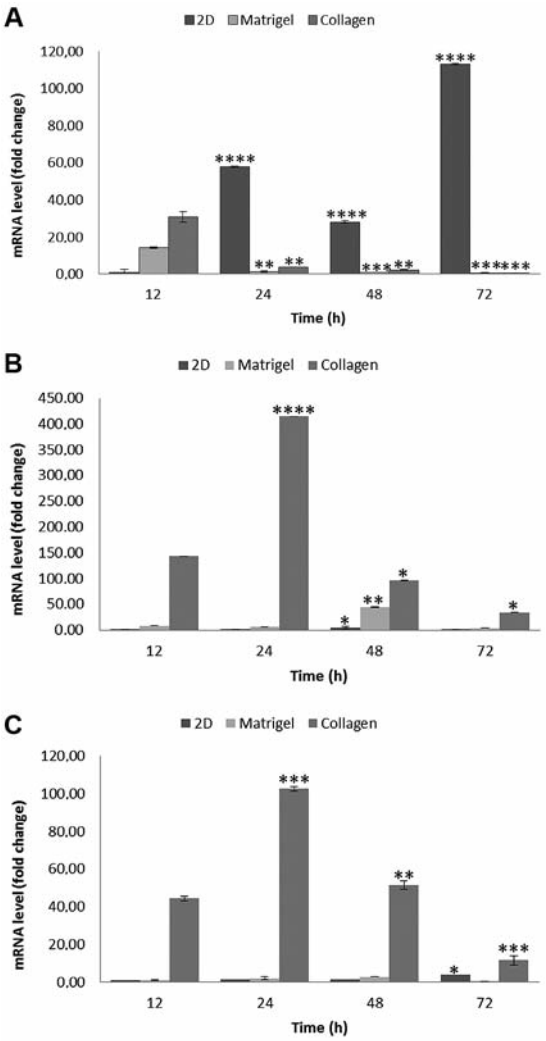

Figure 4. *Expression of mRNA of neuronal nitric oxide synthase (nNOS; A) induced nitric oxide synthase (iNOS; B) and nitric oxide synthase 1AP (NOS1AP; C) in 143B human osteosarcoma cells seeded in monolayers (2D) or in 3D scaffolds (Matrigel and collagen) measured by real-time polymerase chain reaction. The results were normalized to the ribosomal protein L 37a (RPL37A) content. Data are shown as the mean±SD of three independent experiments (N=6 replicate cultures). The absence of an error bar denotes a line thickness greater than the error. *p<0.01, **p<0.001, ***p<0.0001 and ****p<0.00001 versus control (cells at 12 h).*

Transcripts of nNOS showed a relatively high expression in monolayers as of 24 h onwards, which was opposite in the case of both 3D environments. In Matrigel, the *nNOS* mRNA levels were decreased by ~37-fold after 24 h, ~31-fold after 48 h and ~147-fold after 72 h, whereas in collagen by ~15-fold after 24 h, ~12-fold after 48 h and ~163-fold after 72 h. Interestingly, two other genes, *iNOS* and *NOS1AP*, had quite different expression patterns, with strong elevation in 3D scaffolds. This up-regulation was particularly noticeable in collagen, with changes of ~780-fold after 24 h, ~20-fold after 48 h and ~18-fold after 72 h for *iNOS* and by ~68-fold after 24 h, ~33-fold after 48 h and ~3-fold after 72 h for *NOS1AP* (Figure 4).

As shown in Figure 5, the expression of *CAT, SOD1* and *SOD* was also regulated by cell culture conditions. Transcripts of *CAT* were slightly up-regulated in collagen after 24 h (by ~3-fold when compared to the monolayer), but at the final time point showed a modest down-regulation in

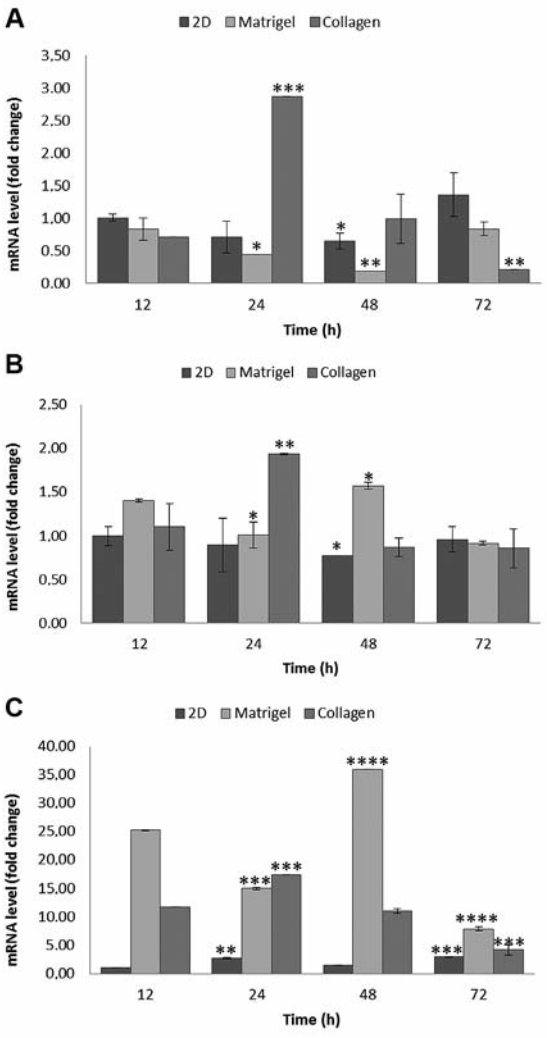

Figure 5. *Expression of mRNA of catalase (CAT; A), superoxide dismutase 1 (SOD1; B) and superoxide dismutase 2 (SOD2; C) in 143B human osteosarcoma cells seeded in monolayers (2D) or in 3D scaffolds (Matrigel and collagen) measured by real-time polymerase chain reaction. The results were normalized to the ribosomal protein L 37a (RPL37A) content. Data are shown as the mean±SD of three independent experiments (N=6 replicate cultures). The absence of an error bar denotes a line thickness greater than the error. *p<0.01, **p<0.001, ***p<0.0001 and ****p<0.00001 versus control (cells at 12 h).*

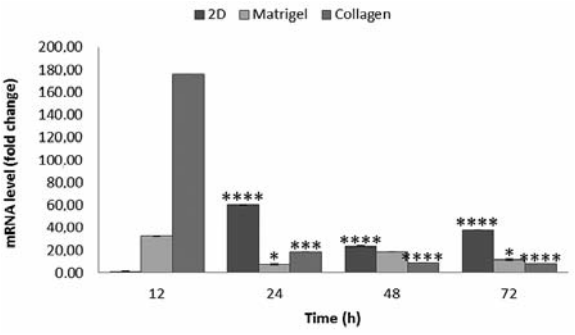

Figure 6. *Expression of mRNA of hypoxia-inducible factor 1 alpha (HIF1A) in 143B human osteosarcoma cells seeded in monolayers (2D) or in 3D scaffolds (Matrigel and collagen) measured by real-time polymerase chain reaction. The results were normalized to the ribosomal protein L 37a (RPL37A) content. Data are shown as the mean±SD of three independent experiments (N=6 replicate cultures). The absence of an error bar denotes a line thickness greater than the error. *p<0.01, ***p<0.0001 and ****p<0.00001 versus control (cells at 12 h).*

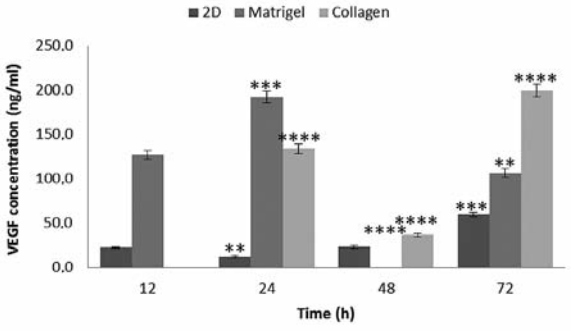

Figure 7. *Concentration of vascular endothelial growth factor (VEGF) in cell culture media of 143B human osteosarcoma cells cultured in monolayers (2D) or in 3D scaffolds (Matrigel, collagen) measured by enzyme- linked immune assay. The relative differences in VEGF concentrations between the samples are clear. Values are the mean±SD of three independent experiments (N=6 replicate cultures). The absence of an error bar denotes a line thickness greater than the error. **p<0.001, ***p<0.0001 and ****p<0.00001 versus control (cells at 12 h).*

3D by ~1.6-fold in Matrigel and by ~7-fold in collagen. *SOD2* expression was elevated in 3D environments at all time points, with the strongest up-regulation in Matrigel after 48 h (by ~24-fold). On the other hand, transcripts of *SOD1* were steadily expressed by 143B cells in all three environments throughout 72 h. Interestingly, expression of mRNA of *HIF1A* was elevated in 3D after 12 h of cultivation (by ~33-fold in Matrigel and ~176-fold in collagen), but then was relatively higher in monolayers, with down-regulation by ~3-fold in Matrigel and ~4-fold in collagen at the final time point (Figure 6).

Concentration of VEGF in cell culture media. In the present study, ELISA was used for the measurement of the VEGF concentration in cell culture media of cells cultivated in three distinct environments (2D, in Matrigel, in collagen). As

shown in Figure 7, the VEGF concentration in 143B cells medium was generally higher in 3D cultures than in monolayers at all time points. After 12 h, the concentration was the highest in Matrigel (127.1 ng/ml). This was also the case after 24 h of cultivation (192.2 ng/ml in Matrigel), but at this time point, the VEGF concentration in collagen-seeded cultures was also remarkably high (133.9 ng/ml). At the final time point, the VEGF concentration was very high in collagen (199.6 ng/ml).

Discussion

Since nitro-oxidative stress in cell cultures remains an under-appreciated issue, the aim of the present study was to examine response of OS 143B cells to a sudden environmental change after transfer to 3D cell culture. The influence of exposure to a spatial environment that provides limited oxygen exposure and allows for active intercellular communication was investigated in terms of nitro-oxidative stress markers expression and compared to the standard 2D cell cultures. The advantages of 143B cells include high homogeneity, fast growth rate and elevated proliferative potential (17). Herein, the cell cultures were established within collagen type I and Matrigel. We have shown the viability of 143B cells was initially maintained at similar levels in all three types of environments (2D, collagen I and Matrigel). Interestingly, at 72 h, we observed diminished cellular viability in monolayers, which may be caused by rapid proliferation high confluence and contact inhibition of 143B cells. Furthermore, the cells embedded within collagen demonstrated the most complex intracellular interactions, *e.g.* the formation of junctions between some separated cells. In a sense, collagen-seeded cultures resembled dendritic osteocytes constituting spacious networks of cells when the ECM is present (18). In contrast, the cells cultured in Matrigel were round or nearly spherical and did not seem to proliferate. Interestingly, a recent study demonstrated that various ECM components, including collagen I, IV and laminin, can exert different effects on human cell adhesion, survival and functionality (19). From these observations, collagen seems to be a better mimic of the ECM for cultivation of osteoblast-like cells for bone tissue engineering applications.

In order to find further molecular explanations of our observations, we compared the effects of 2D and 3D cellular environment on the levels of nitro-oxidative stress. We analyzed the most important factors involved in nitro-oxidative stress response being targets for anticancer therapy namely: major HSPs, NOSs (hemoproteins catalyzing reaction of nitric oxide generation), CAT (an enzyme catalyzing the decomposition of hydrogen peroxide), and SOD (SOD1, SOD2, enzymes decomposing free superoxide radicals) (20).

One of the hallmarks of stress is the expression of HSPs in response to accumulation of misfolded proteins (20). Interestingly, both collagen and Matrigel environment showed protective effects on 143B cells in terms of HSPs response. This observation indicates that some of the major components of the cellular stress response mechanism were decreased in cells cultured in 3D environments, which was the contrary in cells cultured in monolayers. On the other hand, down-regulation of oxidative stress-related genes in 3D cultures was not apparent. Only the expression of CAT was significantly reduced in 3D after 72 h, with the most significant effect in collagen. Alternatively, *SOD1* and *SOD2* mRNA levels seemed up-regulated in the 3D environments compared to 2D. These results point out that 143B cells in 3D were subjected to strong oxidative stress, but apparently it did not result in protein damage or misfolding, thus the basal level of HSPs was decreased in 3D cultures in comparison to 2D. Interestingly, the expression of *nNOS* was significantly reduced in both Matrigel and collagen during the course of experiments. In addition, we found the *nNOS* levels to be low in 3D environments, contrary to the *iNOS* levels. Such a contradictive nitro-oxidative stress response might result from a fact that *nNOS* is constitutively expressed at very low levels in bone cells (16), whereas *iNOS* expression is enhanced in bone cells due to hypoxic or inflammatory conditions (21), and iNOS is usually the predominant nitric oxide producer (22). Interestingly, VEGF concentrations in 143B cells culture media were the highest in 3D environments, reaching maximal concentrations in collagen after 72 h. It could be postulated that HIF1A plays an important role as inducer of *iNOS* and *VEGF* in a 3D environment (23-25).

From these observations, it is not clear whether 3D scaffolds, particularly collagen and Matrigel, can reduce oxidative stress levels in cell cultures for bone tissue engineering. As mentioned above, one major problem in 3D tissue cultures is the hampered oxygen supply (12, 13). 3D scaffolds seem to create strong hypoxic environments in cell cultures that trigger molecular responses in osteoblasts leading to cell differentiation and survival (*e.g.* growth factor signaling). Unfortunately, continuous 3D cultures of cell lines might not constitute a good model for bone tissue engineering in spatial cell cultures, as they are highly sensitive to hypoxia, and hypoxic conditions can induce oxidation of the cellular environment.

Such cultures *in vitro* are associated with relevant oxygen gradients, which can be the cause of inhomogeneous tissue quality (26). *In vivo*, the distance between cells and capillaries that provide oxygen and nutrients ranges from 20 to 200 mm (27). *In vitro*, sufficient nutrition and oxygenation of cells by diffusion is limited to a distance of 100-200 μm (28, 29). Evidently, such oxygen-inhomogeneous cultures do not display a uniform response to oxidation. In fact, oxygen

concentrations affect various cellular mechanisms, including the cell cycle, proliferation and apoptosis (30, 31). Several studies provided proof that the process of osteogenic differentiation is also highly dependent on the oxygen level (32-34), and hypoxia was shown to impact onbone development (30). In consequence, maintenance of stable and even oxygenation in bone tissue engineering is a requirement for generating homogeneous tissues.

Conclusion

Taken together, our data demonstrate the complexity of nitro-oxidative stress biology with regard to the use of novel 3D scaffolds in bone tissue engineering approaches. As demonstrated, commercial cell lines might not constitute a good model of 3D cultures for bone tissue engineering, as they are highly sensitive to hypoxia, and hypoxic conditions can induce oxidation of the cellular environment.

Acknowledgements

This research project received funding from the Foundation for Polish Science (HOMING PLUS/2012-5/11).

References

1 Justice BA, Badr NA and Felder RA: 3D cell culture opens new dimensions in cell-based assays. Drug Discov Today *14*: 102-107, 2009.

2 Tortelli F and Cancedda R: Three-dimensional cultures of osteogenic and chondrogenic cells: a tissue engineering approach to mimic bone and cartilage *in vitro*. Eur Cell Mater *17*: 1-14, 2009.

3 Ferrera D, Poggi S, Biassoni C, Dickson GR, Astigiano S, Barbieri O, Favre A, Franzi AT, Strangio A, Federici A and Manduca P: Three-dimensional cultures of normal human osteoblasts: proliferation and differentiation potential *in vitro* and upon ectopic implantation in nude mice. Bone *30*: 718-725, 2002.

4 Fennema E, Rivron N, Rouwkema J, van Blitterswijk C and de Boer J: Spheroid culture as a tool for creating 3D complex tissues. Trends Biotechnol *31*: 108-115, 2013.

5 Lutolf MP and Hubbell JA: Synthetic biomaterials as instructive extracellular microenvironments for morphogenesis in tissue engineering. Nat Biotechnol *23*: 47-55, 2005.

6 Kasten P, Vogel J, Luginbühl R, Niemeyer P, Weiss S, Schneider S, Kramer M, Leo A and Richter W: Influence of platelet-rich plasma on osteogenic differentiation of mesenchymal stem cells and ectopic bone formation in calcium phosphate ceramics. Cells Tissues Organs *183*: 68-79, 2006.

7 Masi L, Franchi A, Santucci M, Danielli D, Arganini L, Giannone V, Formigli L, Benvenuti S, Tanini A and Beghè F: Adhesion, growth, and matrix production by osteoblasts on collagen substrata. Calcif Tissue Int *51*: 202-212, 1992.

8 Yamanouchi K, Satomura K, Gotoh Y, Kitaoka E, Tobiume S, Kume K and Nagayama M: Bone formation by transplanted human osteoblasts cultured within collagen sponge with dexamethasone *in vitro*. J Bone Miner Res *16*: 857-867, 2001.

9 Kleinman HK and Martin GR: Matrigel: basement membrane matrix with biological activity. Semin Cancer Biol *15*: 378-386, 2005.

10 Kasten P, Vogel J, Beyen I, Weiss S, Niemeyer P, Leo A and Lüginbuhl R: Effect of platelet-rich plasma on the *in vitro* proliferation and osteogenic differentiation of human mesenchymal stem cells on distinct calcium phosphate scaffolds: the specific surface area makes a difference. J Biomater Appl *23*: 169-188, 2008.

11 Pampaloni F, Reynaud EG and Stelzer EH: The third dimension bridges the gap between cell culture and live tissue. Nat Rev Mol Cell Biol *8*: 839-845, 2007.

12 Wendt D, Stroebel S, Jakob M, John GT and Martin I: Uniform tissues engineered by seeding and culturing cells in 3D scaffolds under perfusion at defined oxygen tensions. Biorheology *43*: 481-488, 2006.

13 Arkudas A, Beier JP, Heidner K, Tjiawi J, Polykandriotis E, Srour S, Sturzl M, Horch RE and Kneser U: Axial prevascularization of porous matrices using an arteriovenous loop promotes survival and differentiation of transplanted autologous osteoblasts. Tissue Eng *13*: 1549-1560, 2007.

14 Farnsworth N, Bensard C and Bryant SJ: The role of the PCM in reducing oxidative stress induced by radical initiated photoencapsulation of chondrocytes in poly(ethylene glycol) hydrogels. Osteoarthritis Cartilage *20*: 1326-1335, 2012.

15 Gorska M, Kuban-Jankowska A, Antoniewicz J and Wozniak M: Effect of 2-methoxyestradiol on dephosphorylation of neuronal nitric oxide synthase in osteosarcoma 143B Cells. An *in vitro* study. J Clin Toxicol *5*: 240, 2015.

16 Gorska M, Kuban-Jankowska A, Zmijewski M, Marino Gammazza A, Cappello F, Wnuk M, Gorzynik M, Rzeszutek I, Daca A, Lewinska A and Wozniak M: DNA strand breaks induced by nuclear hijacking of neuronal NOS as an anticancer effect of 2-methoxyestradiol. Oncotarget *6*: 15449-15463, 2015.

17 Subramaniam M, Jalal SM, Rickard DJ, Harris SA, Bolander ME and Spelsberg TC: Further characterization of human fetal osteoblastic hFOB 1.19 and hFOB/ER alpha cells: bone formation *in vivo* and karyotype analysis using multicolor fluorescent *in situ* hybridization. J Cell Biochem *87*: 9-15, 2002.

18 Karsdal MA, Larsen L, Engsig MT, Lou H, Ferreras M, Lochter A, Delaissé JM and Foged NT: Matrix metalloproteinase-dependent activation of latent transforming growth factor-beta controls the conversion of osteoblasts into osteocytes by blocking osteoblast apoptosis. J Biol Chem *277*: 44061-44067, 2002.

19 Daoud J, Petropavlovskaia M, Rosenberg L and Tabrizian M: The effect of extracellular matrix components on the preservation of human islet function *in vitro*. Biomaterials *31*: 1676-1682, 2010.

20 Gorska M, Marino Gammazza A, Zmijewski MA, Campanella C, Cappello F, Wasiewicz T, Kuban-Jankowska A, Daca A, Sielicka A, Popowska U, Knap N, Antoniewicz J, Wakabayashi T and Wozniak M: Geldanamycin-induced osteosarcoma cell death is associated with hyperacetylation and loss of mitochondrial pool of heat shock protein 60 (hsp60). PLoS One *8*: e71135, 2013.

21 van't Hof RJ, Macphee J, Libouban H, Helfrich MH and Ralston SH: Regulation of bone mass and bone turnover by neuronal nitric oxide synthase. Endocrinology *145*: 5068-5074, 2004.

22 Tan F, Naciri M and Al-Rubeai M: Osteoconductivity and growth factor production by MG63 osteoblastic cells on bioglass-coated orthopedic implants. Biotechnol Bioeng *108*: 454-464, 2011.

23 Komatsu DE and Hadjiargyrou M: Activation of the transcription factor HIF-1 and its target genes, VEGF, HO1, iNOS, during fracture repair. Bone *34*: 680-688, 2004.
24 Jozkowicz A, Cooke JP, Guevara I, Huk I, Funovics P, Pachinger O, Weidinger F and Dulak J: Genetic augmentation of nitric oxide synthase increases the vascular generation of VEGF. Cardiovasc Res *51*: 773-783, 2001.
25 Kimura H and Esumi H: Reciprocal regulation between nitric oxide and vascular endothelial growth factor in angiogenesis. Acta Biochim Pol *50*: 49-59, 2003.
26 Volkmer E, Drosse I, Otto S, Stangelmayer A, Stengele M, Kallukalam BC, Mutschler W and Schieker M: Hypoxia in static and dynamic 3D culture systems for tissue engineering of bone. Tissue Eng Part A *14*: 1331-1340, 2008.
27 Muschler GF, Nakamoto C and Griffith LG: Engineering principles of clinical cell-based tissue engineering. J Bone Joint Surg Am *86-A*: 1541-1558, 2004.
28 McClelland RE and Coger RN: Use of micropathways to improve oxygen transport in a hepatic system. J Biomech Eng *122*: 268-273, 2000.
29 Carrier RL, Rupnick M, Langer R, Schoen FJ, Freed LE and Vunjak-Novakovic G: Perfusion improves tissue architecture of engineered cardiac muscle. Tissue Eng *8*: 175-188, 2002.
30 Wang Y, Wan C, Deng L, Liu X, Cao X, Gilbert SR, Bouxsein ML, Faugere MC, Guldberg RE, Gerstenfeld LC, Haase VH, Johnson RS, Schipani E and Clemens TL: The hypoxia-inducible factor alpha pathway couples angiogenesis to osteogenesis during skeletal development. J Clin Invest *117*: 1616-1626, 2007.
31 Malda J, Klein TJ and Upton Z: The roles of hypoxia in the *in vitro* engineering of tissues. Tissue Eng *13*: 2153-2162, 2007.
32 Salim A, Nacamuli RP, Morgan EF, Giaccia AJ and Longaker MT: Transient changes in oxygen tension inhibit osteogenic differentiation and Runx2 expression in osteoblasts. J Biol Chem *279*: 40007-40016, 2004.
33 Potier E, Ferreira E, Andriamanalijaona R, Pujol JP, Oudina K, Logeart-Avramoglou D and Petite H: Hypoxia affects mesenchymal stromal cell osteogenic differentiation and angiogenic factor expression. Bone *40*: 1078-1087, 2007.
34 Malladi P, Xu Y, Chiou M, Giaccia AJ and Longaker MT: Effect of reduced oxygen tension on chondrogenesis and osteogenesis in adipose-derived mesenchymal cells. Am J Physiol Cell Physiol *290*: C1139-1146, 2006.

Received September 20, 2015
Revised November 7, 2015
Accepted November 23, 2015